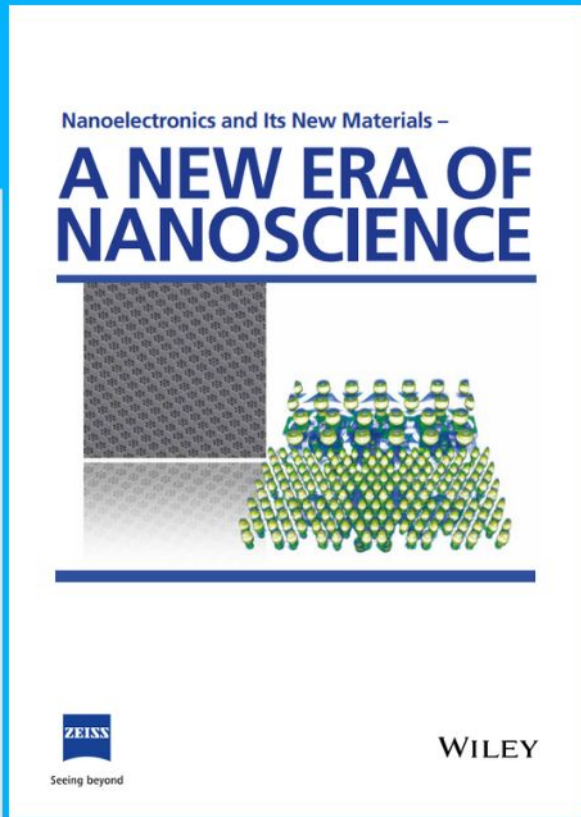




Nanoelectronics and Its New Materials – A NEW ERA OF NANOSCIENCE



Discover the recent advances in electronics research and fundamental nanoscience.

Nanotechnology has become the driving force behind breakthroughs in engineering, materials science, physics, chemistry, and biological sciences. In this compendium, we delve into a wide range of novel applications that highlight recent advances in electronics research and fundamental nanoscience. From surface analysis and defect detection to tailored optical functionality and transparent nanowire electrodes, this eBook covers key topics that will revolutionize the future of electronics.

To get your hands on this valuable resource and unleash the power of nanotechnology, simply download the eBook now. Stay ahead of the curve and embrace the future of electronics with nanoscience as your guide.



Seeing beyond

WILEY

Fabrication of Glass-Ceramic 3D Micro-Optics by Combining Laser Lithography and Calcination

Giedrius Balčas, Mangirdas Malinauskas, Maria Farsari, and Saulius Juodkazis*

This perspective is an overview of a recent direction in optical 3D printing, where polymerization of crosslinkable materials and nanomaterial fillers can be guided to the final structures and new composites via high temperature annealing (HTA). Defining 3D nano/micro-structures by ultrafast laser direct writing and tailoring their precursor composition with subsequent tunability of the final properties during 750–1500 °C HTA step takes place at the large surface-to-volume ratio conditions favoring efficient pyrolysis and calcination, which are required for exchange of chemical materials/gases between glass/ceramic phase and surrounding. Previously, unexplored inorganic material formation conditions in terms of fast thermal quenching, composition mixing and surface tension guided formation can be harnessed by glass making for creation of new materials endowed with preferable technical properties. An immediate application perspective for a high durability, integrated, and active 3D micro-optics is foreseen.

1. Introduction: Concept of Post-Fabrication High-Temperature Treatment

Multiphoton polymerization has already proved to be a versatile lithography tool for micrometer-sized 3D structuring,^[1] reaching sub-wavelength feature sizes, and offering the possibility to fabricate diverse free-form complex 3D micro-optical components^[2] and even miniaturized optical imaging systems.^[3] The 3D-printed micro-optics technology has transitioned from *the innovators* to *early adopters* technological stage.^[4] Until recently, robust lithography-based additive manufacturing (AM) tools, such as two-photon polymerization (TPP), were limited to using organic or organic-inorganic

hybrid materials due to its fundamental requirement on the organic precursor cross-linking polymerization. At the same time, inorganic materials, particularly SiO₂, due to their common use and already highly established foundation in photonics, optical component and microchannel formation, are highly sought after.


The structuring of ceramic and other inorganic materials has been limited in terms of available fabrication methods and the complexity of structures that can be created in 3D space. Additive manufacturing (AM) methods that enable the flexible structuring of silica are needed to advance the fields of micro-optics, micro-electronics, and micro-electromechanical systems. Fabrication of micro-optics using 3D additive manufacturing (AM) techniques involves considerations of minimal feature size, achievable surface roughness, and printed part geometric complexity. Only a brief overview of various categories of 3D AM techniques for ceramic materials will be presented here, while more comprehensive information can be found in relevant review articles.^[5–7] Although several 3D AM methods are routinely used for larger scale component manufacture, such as light induced polymerization based methods employing UV irradiation: StereoLithography (SLA),^[8,9] Digital Light Processing (DLP),^[10–12] deposition methods of Direct Ink Writing (DIW),^[13] Ink Jet Printing (IJP),^[14,15] Fused Deposition Modeling (FDM also known as Fused Filament Fabrication - FFF)^[16,17] and Binder Jetting 3D Printing (BJ3DP)^[18] or layered high-power laser based systems of Laminated Object Manufacturing (LOM)^[19] and Selective Laser Sintering (SLS).^[20] The listed techniques are allowing typical achievable feature sizes of tenths of micrometers^[21–23] to millimeters in dimensions.^[24,25] Ability to create efficient optical

G. Balčas, M. Malinauskas
Laser Research Center, Physics Faculty
Vilnius University
Sauletekio Ave. 10, LT-10223, Vilnius Lithuania

M. Farsari
IESL-FORTH
N. Plastira 100
Heraklion, Crete 70013, Greece

S. Juodkazis
Optical Sciences Centre, School of Science
Swinburne University of Technology
Hawthorn, VIC 3122, Australia
E-mail: sjuodkazis@swin.edu.au

S. Juodkazis
WRH Program International Research Frontiers Initiative (IRFI), Tokyo
Institute of Technology
Nagatsutacho, Midori-ku
Yokohama, Kanagawa 226-8503, Japan

 The ORCID identification number(s) for the author(s) of this article can be found under <https://doi.org/10.1002/adfm.202215230>

© 2023 The Authors. Advanced Functional Materials published by Wiley-VCH GmbH. This is an open access article under the terms of the Creative Commons Attribution License, which permits use, distribution and reproduction in any medium, provided the original work is properly cited.

DOI: 10.1002/adfm.202215230

elements is directly linked to the wavelength for which the optical element is design to function. This makes all of the aforementioned methods only suitable for longer wavelength electromagnetic wave manipulation, such as the elements that have been demonstrated for THz and mm-wave range.^[26–28] In contrast, techniques such as Aerosol Printing (AP),^[29,30] Glancing Angle Deposition (GAD),^[31] Meniscus Printing (MP),^[32] Interference Lithography (IL),^[33] Imprint Lithography (IL) methods^[34–36] and Electron Induced Deposition (EID)^[37,38] are capable of achieving sub-wavelength feature sizes for the visible range optical or photonic components. Among them, only EID has demonstrated the ability to create truly 3D geometries,^[37] while the other techniques have only been shown to produce 1D lattice or 2D extruded structures with varying degrees of spatial control and process repeatability.^[31,39–41] Despite these geometric restrictions, these technologies have been used to create functionalized surfaces for Surface-Enhanced Raman Spectroscopy (SERS)^[42] or chiral metamaterials^[43,44] for use in optical applications. In the case of EID, there are still technological limitations that result in non-linear geometric responses to system parameters and a low printing throughput of approximately 0.8 voxels^{-1} ,^[38] compared to MPL based techniques with values reaching 10^5 voxels^{-1} ^[45] using single and up to 10^6 voxels^{-1} using multiple beams approaches.^[46]

There is a growing demand for the precise control over inorganic materials that goes beyond basic 2D extruded shapes. This need is particularly evident in high-quality refractive optics-based imaging systems that require multi-element systems to minimize optical and chromatic aberrations.^[47,48] Additionally, interest in 3D chiral geometries have been demonstrated^[40] to elicit a stronger chiro-optical response in respective chiral-optical elements. 3D structures can create more pronounced spatial asymmetries, resulting in greater differences in the interaction of left- and right-circularly polarized light with the structures.^[49] Furthermore, ability to fabricate compound multi-element systems have also attracted attention in meta-surface fabrication, offering more functional degrees of freedom.^[50] For instance, one of beneficial factors of moving to 3D is the ability to form polarization independent components, as demonstrated by Zhan et al.,^[51] and to achieve wavelength or angle independent meta-surface systems.^[52] The 3D AM technology benefit can also be harnessed in the case of photonic integrated circuit (PIC) designs. High spatial complexity allows to create non-trivial highly-integrated miniature opto-mechanical systems.^[53]

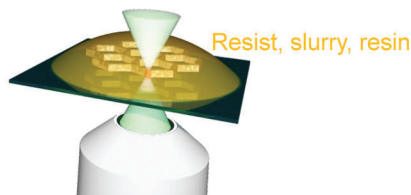
Currently, Multi-Photon Lithography is the most versatile AM technology that has the ability to form true 3D complex multi-element structures in the nano/micro scale, which is needed to access a wide field of micro-optics.^[54] This technology has been successfully demonstrated in the fabrication of optical sensing micro-systems, as one demonstrated by Zhang et al.,^[55] compound objective imaging systems,^[56] or even completely suspended geometries,^[45,57] including examples as Xia et al. demonstrated micro-nanomachines.^[58]

While there have been breakthroughs in the use of lithography for inorganic material structuring, such as the recent work of Duan et al., who demonstrated inorganic structuring on the nanoscale ($<30 \text{ nm}$),^[59] the ability to achieve high levels of form control at nano/micro feature scale has not yet been demonstrated. In addition, the method described by these authors has

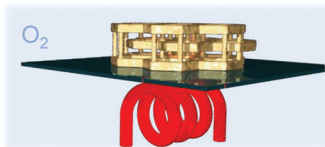
intrinsic limitations in terms of the possible height of prepolymer layers, which prevents the manufacture of true 3D freestanding geometries.

Emerging heat treatment post-processes for MPL, either a calcination (a complete removal of organic fraction of the formed structure) or a pyrolysis (heating of organic material in the absence of oxygen), have the enabling potential to structure inorganic materials at micro-/nano-scales via AM means,^[60] example given in **Figure 1**. Polymer precursor transformation into ceramics through a heat treatment process, known as thermal conversion, resulting in the removal of the organic components and the formation of a ceramic network is widely researched in the case of structures with dimensions much higher than $100 \mu\text{m}$ mark, in the matured field of Polymer Derived Ceramics (PDCs).^[61] Organosilicon polymers conversion to ceramic materials has been investigated since 1960s as a promising route of producing ceramics for various applications;^[62] the resulting inorganic materials have attractive properties such as high-temperature stability, oxidation resistance, and exceptional mechanical properties, and has been integrated together with various AM methods, each offering individual advantages.^[5,63] High throughput and build volume can be realized using material extrusion based techniques such as direct ink writing, fused deposition molding and inkjet printing. These techniques place minimal restrictions on the material selection but are heavily restricted in achievable feature sizes ($100 \mu\text{m}$ to millimeters). In the case of higher resolution components fabrication, lithography based techniques such as interference lithography, digital light processing (DLP) and stereolithography (SLA) are seen as most versatile. However, even these methods are limited by their linear absorption triggering photo-activation of precursor materials, which limits their achievable spatial resolutions to being tens-of-micrometers. Whereas, the emerging field of 3D micro-optics require sub-wavelength geometry and at a high fidelity. Here, the MPL, due to its nonlinear light-matter interaction nature, is offering sub-diffractive resolution and decreasing achievable feature sizes down to sub- 100 nm .^[64] Differently than other listed AM techniques, the incorporation of MPL with PDCs is still a highly understudied field with limited understanding of thermal conversion caused material changes (density, porosity, refractive index, geometry preservation), material phase evolution and defect formation. Furthermore, intrinsic difference of moving to micro-/nano-scales leads to new material functionalities that have not been yet researched in the case of classical PDCs. For instance, this scale is sought for photonic devices and sensors, where precise control over material properties and features is critical. Additionally, the integration of MPL with PDCs can open up new possibilities in the fabrication of complex 3D structures, as well as the development of novel material compositions with enhanced properties that until now, were unreachable for traditional MPL methods, for example, lanthanide doped optically active materials and high refractive index inorganic substances.^[65–67] In contrast to purifying the hybrid material into inorganic substance, it allows getting rid of undesired organic ingredients, such as complete removal of harmful residual monomers and toxic as well as coloring photo-initiators. The later ones are also detrimental due to their auto-fluorescence which can negatively affect optical properties or saturate the signal while performing cell micro-imaging in biomedical research fields.^[68]

1) Laser 3D nano-printing (sub – 1 ps)
CNC – Computer Numerical Control



2) Calcination at > 1000°C



3) Glass / Crystalline 3D nano-structure

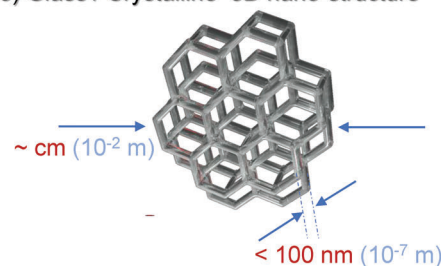


Figure 1. Concept of a 3D printing via computer numerical control (CNC): from a polymer to glass-ceramic through a controlled high temperature annealing in oxygen. Feature sizes in the final workpiece can reach nanoscale ≈ 100 nm features for macro-dimensions of \approx cm, hence, a mesoscale 3D structuring/printing.

Historically HTA implementation as a post-processing tool for MPL was first demonstrated by Pham et al.,^[69] where authors have successfully structured fully SiCN ceramic microstructures with spatial resolution of >400 μ m. This marked a breakthrough of PDCs conjugation with MPL and further led material engineering research for more attractive material compositions for optical use. Pham et al. work was followed by other silicorganic polymer implementation for ceramic materials of SiC, SiOC structuration which have high absorption. Further on, B. Rapp et al. published on the now-commercialized nanocomposite Glassomer polymerization via UV lithography^[70] and later demonstrated structuring through multi-photon lithography.^[71] While the research group has demonstrated the manufacture of silica-like materials with a resolution of tens of micrometres using MPP DLW, this falls behind the achievements in feature sizes capable by traditional MPP methods that are needed for efficient micro-optical and photonic integrated circuit (PIC) systems.^[72,73]

The use of specially designed pre-polymer materials in conjunction with a post-process heat treatment has attracted interest from various research groups as a means of breaking the nano/micro scale feature size barrier for inorganic 3D additive manufacturing processes and expanding the range of structured material properties, including absorption, mechanical strength, chemical and thermal stability, and high refractive index. By elevating the temperature of the material to close or beyond its glass transition temperature, structures composed of glass and/or ceramic phases can be produced. These post-processing methods allow for the application of precise, high resolution polymer structuring in well-established glass material applications. As thermodynamics and kinetics are both intertwined in glass formation, heat treatment opens new toolbox to control glass, especially, where the small volume and cross-section of the structures undergoes fast thermal quenching, reaching under-cooling conditions impossible for bulk materials. New, previously impossible glass formation conditions can be explored, such as those which recently attracted attention in formation of metallic glasses versus their crystalline counterparts of high entropy alloys.^[74,75] and provide much required understanding in still unresolved glass formation (2022 is UNESCO's year of glass). This perspective article aims to summarize current new findings and promising direction emerging in micro-optics and nano-structure experimentation, which eventually will bring understanding of the enigmatic glass formation at increasingly much smaller space domain.

2. Method

A combination of MPL and heat treatment was used as a method to sinter and further lock inorganic materials after they have been encapsulated in a pre-defined organic matrix through the use of direct laser polymerization. Suspension of inorganic compounds in a fixed geometry could be achieved via a number of MPL methods of increasing complexity:

- 3D structures made from resin, consisting inorganic composite materials, using MPL process. Once the structure has been formed, non-crosslinked material was removed using solvent solutions during development process.
- polymerization of a mould structure or structuring via sequence of inversions, that is, material consisting of inorganic precursor was added after the structuring of 3D geometry has been achieved in the previous step.^[76]
- Similar to the case above, hollow structures could be fabricated through sacrificial template method.^[77]

Usually, after the inorganic precursor shaping step, an organic binder material fraction was present, which acts as a matrix for inorganic material encapsulation. To obtain the final fully inorganic material, debinding of organic fraction was performed at elevated temperature, at which its organic fraction was disintegrated. The typical debinding temperatures were above 400 °C^[78,79] and the sample was held at this temperature for a few hours until the organic fraction was completely decomposed and removed.

Further increase in temperature leads to the conversion of either amorphous glass or poly-crystalline phase-mechanically and chemically inert structures, depending on the specific sintering parameters used, such as annealing temperature, heating/quenching rates, and atmosphere. Densification of the material, due to removal of organic fraction, leads to finer dimensions and, in some cases, higher refractive index objects, while maintaining freely produced 3D shape, created with conventional or advanced stereo-lithographic polymerization techniques. Since the refractive index was proportional to the mass density, micro-optical applications are the expected beneficiaries of densification induced by pyrolysis or calcination.

The process of structuring 3D geometries through MPL and heat treatment as a post-processing tool involves several steps. Hybrid organic–inorganic material SZ2080 was chosen as a

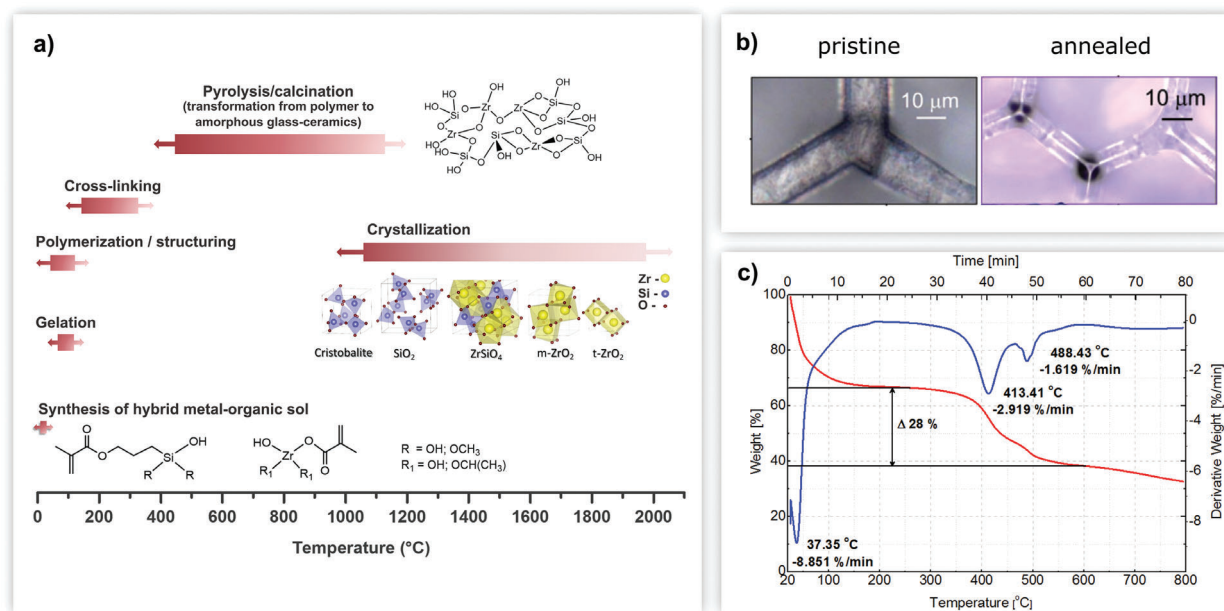


Figure 2. a) Thermal transformation steps from synthesis to crystallization in Si-Zr organometallic system. From the author G. Merkininkaitė with her permission to adapt it for this article.^[81] b) Optical images of 3D-micro scaffolds pre- and post-calcination in 1400 °C atmosphere. Reproduced with permission.^[82] Copyright 2019, Royal Society of Chemistry. c) Thermogravimetric analysis (TGA) data showing weight loss versus temperature. The weight loss was 28% while the observed shrinkage was \approx 40%. The organic component was decomposed and removed by heating. Reproduced under the terms of the CC-BY license.^[83] Copyright 2017, MDPI.

representative example, as it has been widely studied for its ability to undergo such a transformation. Composition of SZ2080 was open and experimentation with photo-initiators tailoring its response to two-photon absorption at specific wavelength of excitation was widely documented^[1,80] (Figure 2).

The first step in this process was the preparation of prepolymer material. In the case of SZ2080, synthesis of a hybrid metal-organic prepolymer was carried out using the sol-gel method. Additionally, gelation may also be required depending on the specific precursors and solvents used. The gelation process typically takes place at temperatures close to the boiling points of the solvents, in most cases- below 120 °C.

The second step was structuring of resist to create an arbitrary 3D architecture using one of the various multi-photon polymerization techniques. Irreversible geometry formation was carried out through the cross-linking of the prepolymer material, creating solvent resistant organic/inorganic networks.

The final step in the process of transforming hybrid organometallic 3D objects into pure inorganic structures was the high-temperature annealing (HTA) treatment of the fabricated 3D structure, which could be made using one of three methods: pyrolysis, calcination, or crystallization. These methods involve the decomposition or rearrangement of chemical bonds, the formation of new chemical bonds, and the removal of the organic component of the material.

Thermo-analytical techniques, Thermo-Gravimetric Analysis (TGA), and Differential Scanning Calorimetry (DSC) were frequently used tools for material change monitoring during the HTA.^[84,85] In the case of hybrid SZ2080 TGA, results given in Figure 2c, two main stages of material removal could be distinguished, corresponding to the material phases when the most

pronounced shrinkage occurs, Figure 2a. First peak, typically below 150 °C, corresponds to the dehydration of the material and evaporation of all solvents encapsulated by the structure.^[86] This step also matches the majority of mass loss, depending on the material could reach values higher than 50%.^[67] Aforementioned material phase change also and marks the point of complete thermal polymerization of residual non-reacted monomers/oligomers, as evidenced by Fourier-Transform Infrared spectroscopy (FTIR) data collected by several research groups.^[84,86,87] Material shrinkage at this step manifest through cross-linking and capillary forces that apply on the structure upon removal of constituent ingredients. A second sudden material mass loss occurs at a higher temperature, once again dependant on the precursors, typically occurring at higher than 400 °C.^[88] At this point, the removal of polymerized organic material was initiated, further increase of temperature leads to no significant mass change, signaling to a major part of organic fraction being disintegrated. In the case of most used precursors, amorphous glass-like phase was achieved at temperatures of up to 1100 °C. The crystallization occurs at even higher temperatures of 1100–1200 °C (could reach up to 2000 °C). It was worth noting, that final properties of polycrystalline material phase was heavily influenced by concentrations of precursors.^[67] High proportion of carbon compounds in the pre-HTA material could also lead to formation of a free-carbon, which usually hinders final structures functionality for optical use.^[81,87] The properties of the resulting structures were influenced by various factors, including the composition of the initial material, the heating temperature and rate of temperature increase, the holding time, and the heating atmosphere composition and pressure. In the case of heating/cooling rate

slow temperature change of around $1\text{ }^{\circ}\text{C min}^{-1}$ was chosen, ensuring removal of gases, such as CO and CO₂ released due to the decomposition of organic moieties, and maintaining homogeneous temperature distribution within the structure, as the residual stresses caused by thermal gradients could induce crack formation.^[88,89] Heating atmosphere and pressure could also heavily affect final material properties.^[90] Vacuum conditions have been shown to reduce probability of entrapped air or gas within the structure.^[88] This leads to structures characterized with low porosity and enhanced density, properties that were required for transparent and low loss materials for optical components.

The annealing process parameters influences resulting ceramic/polycrystalline materials properties: density, porosity, surface roughness, and transparency. It could be tailored by controlling the sintering temperature, duration, heating, and cooling ramps. In the case of MPL formed structures, HTA was typically performed using large volume atmosphere air muffle furnace or inert gas filled tube furnace. However, a number of different sintering methods have been utilized for structures formed through various AM methods, including hot uni-axial or isostatic pressing,^[91,92] ion irradiation,^[93,94] EM wave radiation based- using non-coherent light or laser sources,^[95–97] and chemical vapour deposition based methods of heat delivery.^[98,99]

Laser pyrolysis was one of the promising alternatives to traditional methods to be used in combination of MPL. Added spatially selective heating ability has been used outside of polymer derived ceramics subject, and has been proven to be advantageous for laser micro-machined micro-optical devices. For instance, selective laser beam induced thermal change has been used in conjugation with Direct Laser Writing ablated micro-lenticular lens array surfaces,^[100] for optical fibers it has been used to form Whispering Gallery Mode (WGM) cavities^[101] and evanescent wave coupling enhanced tapered fiber sections.^[102] Laser pyrolysis may eliminate one of the biggest given restrains by HTA-substrate material selection governed integrated optical component incapability limitation.^[89]

The final 3D structure obtained after HTA calcination/pyrolysis has a number of important steps to control evolution of the structure, however, the very first polymerization step was very important. Energy deposition by laser (light) inside the volume of polymerizable material was the initiation step, which leads to a sequence of further physicochemical and structural changes. Next, energy deposition per volume during direct laser writing was defined.

2.1. 3D Energy Deposition during 3D Laser Direct Writing

Photosensitive resist/resin for 3D calcination could be prepared using different photo-polymers, photo-initiators/sensitisers, inorganic fillers, or nanoparticles. Such initial photo-materials could have very different absorption and scattering properties as compared with photo-resists/resins which were highly transparent at visible to NIR spectral range. Also, optical near-field effects between constituent nanomaterials with distinct boundaries/surfaces were contributing to the light field localization on nanoscale with dimensions up to few tens of nanometers. This was a direct consequence of boundary conditions for dielectric

permittivity $D_n \equiv \epsilon E_n$, which has to be continuous through the boundary (for non-conductive materials), where E_n if the normal component of electric E-field of light at the interface and ϵ was the permittivity of material. As a consequence, light intensity of the local field between two surfaces with slightly higher refractive index n_h and lower n_l in between, would be enhanced by a factor $(n_h/n_l)^4$ at the location of lower index; this was due to a fact that intensity $I \propto E^2$ and $\epsilon \equiv (n + i\kappa)^2$ with κ being the imaginary part of the index. Nanoparticles of n_h in photo-polymer n_l would be preferably bound by cross-linking in such an exposure. Manifestation of this near-field light enhancement of laser direct write lithography was demonstrated for polarization controlled nanoscale ablation^[103] and was present in formation of nanoscale ripples in the laser damaged regions inside bulk of transparent materials using ultra-short laser pulses due to self-organization present in multi-scattering environment on a nanoscale.^[104] Recently, self-assembly of plasmonic nanoparticles inside solid state glass was achieved using ultra-short laser pulses and energy deposition via plasmonic near-fields.^[105]

Strongly localized energy deposition down to nanoscale and local temperature increase should not be underestimated in chemical cross-linking reactions which have the exponential Arrhenius character of the reaction rates. In direct laser writing with tightly focused ultra-short laser pulses, in situ characterization of sub-wavelength volumes was a challenge and pump-probe methods were required to probe the focal volume. In fact, pump and two probes at same wavelengths but different angle of incidence was required to recover pair of (n, κ) from a single measurement.^[106] The light-matter interaction was fully known/described when the light intensity I was known together with permittivity (epsilon) $\epsilon = (n - \kappa)^2 + i2n\kappa$ which defines the energy deposition. The n and κ determines portions of light which were reflected and absorbed via the reflectance $R(n, \kappa)$ and absorbance $A(\kappa)$. Since temporal changes of ϵ were described by the electronic excitations/transitions, they follow the intensity envelope of the driving laser pulse. Hence, instantaneous $\epsilon(t)$ determines the energy deposition at the voxel. Changes of ϵ could be regarded as an optical nonlinearity reflective of the cumulative material response in n and κ . Each photo-excited electron contributes a negative part to n (initially positive) and augments κ due to absorption in the continuum of free electronic states. Hence, photo-excitation of material drives $Re[\epsilon] = (n - \kappa)^2 \rightarrow 0$, hence, epsilon-near-zero (ENZ) state.^[107] The ENZ has attracted attention due to the condition of perfect absorber in plasmonics and nanophotonics, when absorbance $A \rightarrow 1$ due to reflectance $R \rightarrow 0$ (for the case when there was not transmittance $T = 0$ and overall energy conservation $A + R + T = 1$). The most efficient energy deposition was taking place when $1 > Re[\epsilon(t)] > 0$ occurring during the laser pulse. This energy deposition into electronic state of material was coupled to ions and atoms at the later stages starting couple of picoseconds later when laser pulse was already left the interaction volume (the voxel in terms of building block in polymerization). This ENZ-state was transient when dielectric medium acquires metallic of plasma-like state, hence, Die-Met.^[108] The strong absorption at ENZ eventually could lead to the dielectric breakdown, which was defined by $Re[\epsilon] \equiv 0$, when all the focal volume was transferred to the ionized state. Only ultra-short laser pulses allow for the required energy deposition control while keeping ENZ state but not transferring to the dielectric breakdown.^[107] At the typical

$\approx 0.2 - 1 \text{ TW cm}^{-2}$ per pulse average intensities, the avalanche ionization was prevalent and easily cause the breakdown for longer pulses since energy deposition was in a runaway mode toward the breakdown.

The above described scenario of the energy deposition was generic and was defined by the ϵ . Since polymerization was volumetric 3D process, account of energy density (per volume) $W_{abs} \text{ J cm}^{-3}$ was the most relevant measure as typically used in additive manufacturing, for example, sintering of metallic powders by kW-lasers where energy deposition was defined by temperature diffusion depth into the subsurface during 3D printing. The volumetric energy density W_{abs} was especially important in the ENZ-state of matter since the axial extent of absorption, the skin depth was $l_s \equiv 1/\alpha$, where the absorption coefficient $\alpha = 4\pi\kappa/\lambda = 2\omega\kappa/c \text{ [cm}^{-1}\text{]}$ was dynamically changing during the pulse as the electron density N_e was increasing; c was speed of light and ω its cyclic frequency. The description of light energy deposition and light-matter interaction via ϵ accounts for optical nonlinearities, saturable absorption, photo-response of a solid-state medium, and electronic excitation. The absorbed energy density $W_{abs} \propto \frac{N_e}{N_{cr}} F_p$,^[11] where $F_p = E_p/\text{Area}$ was fluence per focus area and N_{cr} was the critical density at the wavelength of excitation. For 3D polymerization, energy deposition into the voxel volume was important as it should amount to the required exposure dose in order to retrieve 3D structure from wet-bath development. The dose used in standard photolithography (negative and positive tone resists) by cw-laser of UV-lamp exposures was 0.1 J cm^{-2} for high-contrast definition of patterns,^[109] while the highest sensitivity was at $20\text{--}80 \text{ mJ cm}^{-2}$ dose window. Similar doses have to be accumulated for 3D fs-laser polymerization via a non-linear energy deposition at the transparency window of photoresist matrix materials as well as photo-initiators doped at typical mM concentrations ($\approx 0.1\%$ by molecular number density). It was previously shown,^[80] that by use of high $\approx \text{TW cm}^{-2}$ intensity fs-laser pulses, a high sub-wavelength resolution 3D polymerization could be achieved without photoinitiators since the avalanche absorption of the matrix polymer (99.9% by number density) becomes dominant in the free carrier generation rather than 0.1% of photoinitiator excited via a low probability multi-photon process. Regardless of the 3D crosslinking mechanism, 3D polymerized structures undergo the next calcination step which has different peculiarities and methods of control as is discussed below.

It was noteworthy, that the energy deposition into skin depth discussed here for the 3D laser polymerization manifests itself in subtractive 3D processing by ablation. In the burst mode with small pulse energy and high repetition rate of MHz-to-GHz (in the burst),^[110] the delivered energy could be optimized for the most precise 3D removal of material. The removal rate was found dependent on the pulse energy E_p with characteristic second order *slope* = 2,^[110] which was characteristic of the direct absorption by photo-excitation of electrons according to $W_{abs} \propto \frac{N_e}{N_{cr}} F_p \propto F_p^2$ since $N_e \propto F_p$ as observed in the experiment.^[110]

3. Material Properties and Performance

The materials traditionally used for multi-photon lithography are pure organic and hybrid materials; these classes of materi-

als offer a lot of flexibility, however, they also have some limitations: photopolymers have in general low refractive index (RI) and are soft (low Young's modulus). In addition, polymers are more susceptible to thermal and chemical damage. The development of calcination and pyrolysis as post-processing offers the opportunity to address these issues and develop inorganic structures with superior properties to organic or hybrid ones (Figure 3).

In the following paragraphs, we will describe the materials used in order to produce 3D micro- and nano-architected structures for applications in micro-optics with properties beyond what can be achieved using materials with organic functionalities. Hybrid materials are referred to as chemically stable sol-gel synthesized pre-polymers, whereas composites indicate precursor consisting of organic precursors with doped inorganic nanoparticles (typically of five to tenths of nanometers in dimensions).

3.1. Geometry Distortion and Feature Size

Critical material composition and characteristics, such as shape changes, can be perceived as additional obstacles that must be overcome. Material shrinkage due to organic fraction disintegration has been named as a leading limiting factor for the precise manufacture of micro-optical elements.^[113] On the other hand, these new features can be exploited to achieve higher efficiency in structural fictionalization (surface smoothing, lattice periodicity reduction, refractive index increase, etc.). Thus, shrinkage can be seen as both either a positive or a negative aspect of heat treatment. In order to minimize the shrinkage one way is to use precursors with a high percentage of inorganic fraction. Hong et al.^[113] demonstrated the structurization of high inorganic fraction hybrid material named liquid silica resin (LSR). The authors presented glass microlenses and grating structures with ultra-high fidelity geometries and surface roughness R_a values below 6 nm, while maintaining a non-deformed final structure shape and shrinkage below 20% owing to the high inorganic content in the precursor. Desponds et al.^[78] have proposed another approach - the use of ultra-small (5 nm) stabilized ZrO_2 nanoparticles incorporated into the organics precursor. The latter inevitably leads to a reduction in the weight and volume loss owing to the heat treatment.

Observed ultra high fidelity and low surface roughness structures is a technologically promising characteristic of the HTA processed materials. Low surface roughness comes as an added benefit, whereas different micro-optic ultrashort laser direct write fabrication techniques as Selective Laser Etching (SLE) or ablation require additional steps as these techniques create surfaces with roughness values typically being greater than 40 nm.^[114,115] High control of surface roughness is vital in the production of low loss optical components as micro-lenses or total internal reflection based systems as WGM resonators, as in the case of negligible material absorption, it typically accounts for a majority of optical component losses.

Contrary to previously mentioned works, several research groups have recently demonstrated that high temperature purposely induced material shrinkage can be utilized as a post-processing method for achieving reliable and controllable

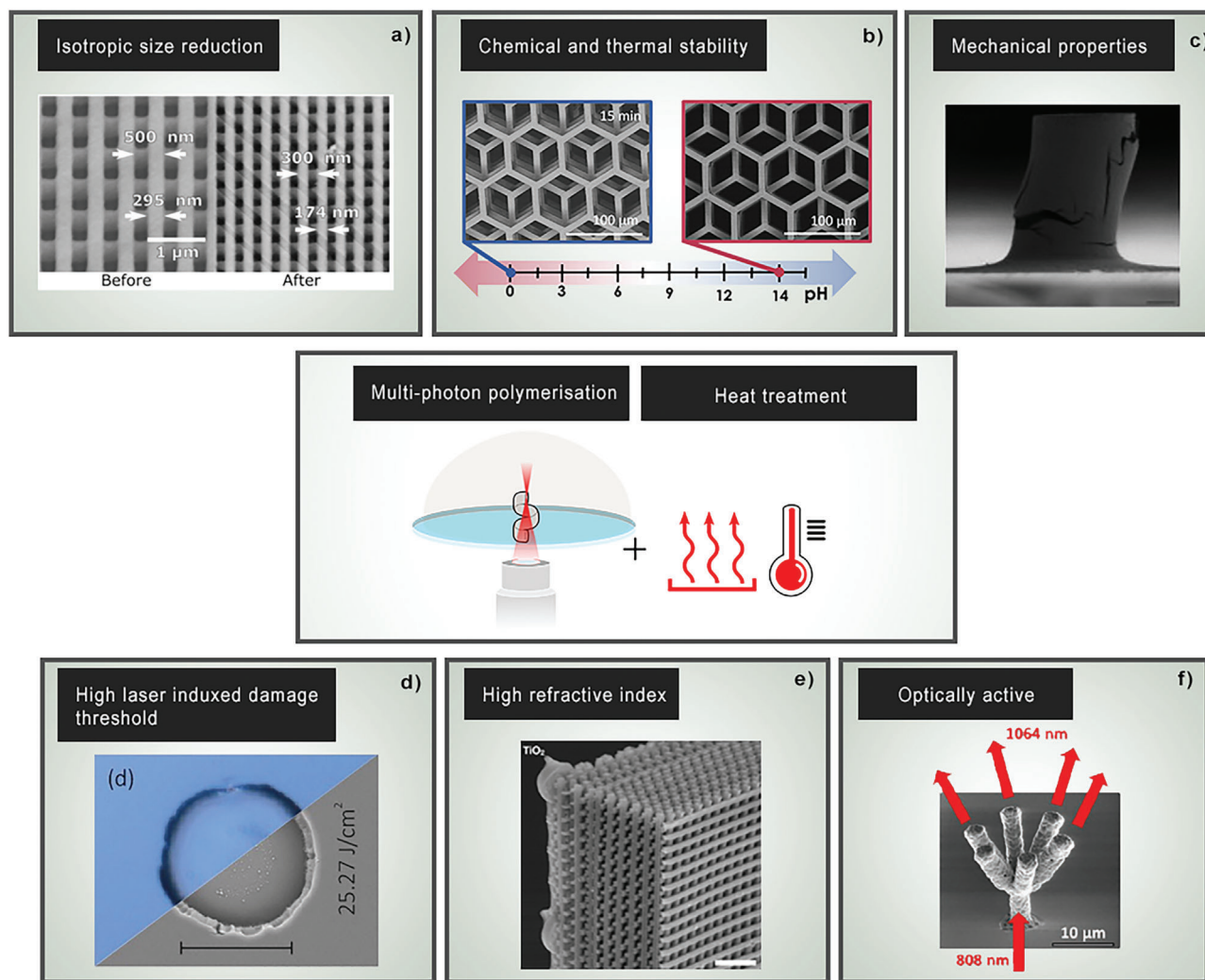


Figure 3. Beyond organic 3D structures. a) SEM graph of a photonic crystal periodic lines prior to and after pyrolysis. Reproduced under the terms of the CC-BY license.^[83] Copyright 2017, MDPI. b) Resistance of ceramic/crystalline 3D nano/micro-derivatives to aggressive chemicals. From the author G. Merkininkaitė with her permission to adapt it for this article.^[81] c) Mechanical Characterization of SiOC Micropillars. Reproduced with permission.^[111] Copyright 2019, Elsevier. d) DIC (colored triangles) and SEM (gray triangles) images of the laser-induced damage morphology of the photosensitized SZ2080 thin film. Reproduced with permission.^[112] Copyright 2015, Elsevier. e) Representative TiO₂ woodpile architectures after calcination at 750–900 °C, scale bar is 2 μm. Reproduced with permission.^[65] Copyright 2020, ACS Publications. f) SEM image of printed light splitter after heating to 1500 °C, the illustration describe the excitation of the structure by a laser at 808 nm wavelength from the bottom, and the emission from the structure at a wavelength of 1064 nm. Reproduced with permission.^[67] Copyright 2020, John Wiley and Sons.

reduction in structural feature sizes. In fact, the use of material shrinkage to achieve a higher resolution of the MPL process has been attempted by other methods as well. For example, team of Xie et al. used so-called nanoprinting-at-expansion/employments-at-recovery strategy, which utilizes pre-stretched elastomeric PDMS substrates that after MPL structuring, are contracted. Thus, avoiding redundant polymerization of adjacent exposures at a short distance, and achieving deep sub-diffraction scale (up to 96 nm) packing of adjacent geometries. Similarly several research groups have demonstrated implosion fabrication techniques,^[116,117] using hydrogel materials as a volumetric scaffolds. Dehydrated hydrogels can shrink in size by the factor of 10–20 times, severely downscaling MPL structured material within them and reaching high packing with resolution

in nm-scale. Using HTA in conjunction with MPL, similar effect can be achieved, however, in this case, the improvement of the functionality of the structures is not accompanied by the negative limitation of the choice of material. Its rather the opposite - improving its technologically preferable properties offered by ceramic/crystalline substances.

Gailevičius et al. have demonstrated 3D woodpile structure resolution reduction of 40% due to the calcination out of SZ2080 material.^[83] In the case of pentaerythritol triacrylate (PETA) based IP-Dip^[118] materials even higher shrinking factor of 78% have been achieved on non-individual geometries through pyrolysis.^[87] In cases of hybrid and non-colloidal resins, shrinkage is isotropic and repeatable, meaning no additional deformation compensations methods have to utilized.

This is extremely favorable for all types of phase modulation optical devices as diffractive optical elements, kinoforms or recently demonstrated birefringent optical retarders.^[119–122] In the case of discrete multi-level phase elements, isotropic shrinkage reduces achievable pixel sizes, reducing scattering losses, and increasing resolution of the devices, most notably reducing the height of individual steps in longitudinal direction. In the case of birefringent retarders or photonic devices, reduction in size, allows to achieve sub-wavelength periodicity lattices, needed for efficient single diffraction order operation throughout visible range.

As a method for feature reduction, thermal material annealing, in contrast to stimulated emission depletion (STED^[123,124]) microscopy-based MPL techniques, can be easily incorporated into currently used MPL systems. Thus, thermal post-processing is not limiting the throughput as it is compatible with the use of already existing rapid printing machinery utilizing galvanometric scanners and/or beam modulation systems, like spatial light modulators or digital micro-mirror devices.^[45,125–127]

3.2. Material Resilience

The elimination of organic fraction from the hybrid material via the use of heat treatment as the route for the fabrication of ceramic 3D structures has been already demonstrated as offering several distinct benefits. It includes improved chemical and thermal stability, higher laser-induced damage thresholds (LIDT), and increased mechanical strength. A recently published study by Merkininkaitė et al. have explored post HTA structure resistance to harsh environmental parameters. The fabricated 3D scaffold structures made from SZ2080 and annealed at up to 1000 °C proved to be immune throughout the temperatures ranging from –200 to 1000 °C. It exhibited no apparent material shrinkage, swelling or structural defect formation (crack formation, detachment from the substrate, or delamination). Furthermore, the same structures were tested in the presence of highly oxidising and aggressive chemical solvent–piranha solution. Compared to polymeric counterparts, the calcinated structures showed no structural difference after immersion and shaking it in ultra-sonic bath. Such material resiliency to environmental parameters in combination with MPL offered functions via freely chosen geometry open a way to widely applicable and durable optical elements, without any loss in design limitations. This makes them ideal for use in optical sensing applications which has been continuously advancing field frequently utilizing MPL as a fast complex geometry prototyping tool.^[128] Currently demonstrated metrology systems made using MPL, for example Kim et al. novel surface-enhanced Raman spectroscopy micro sized system^[129] or integrated Mach-Zehnder interferometer developed by Qi et al.^[130] could be adapted for multi-element micro scale metrology systems working in so far inaccessible high/low temperature or aggressive chemical environments. Increase of interest in ultrashort (pico/femto-second) pulse laser systems demands for micro-optical components that can handle high peak powers and fluences. To this date (end of 2022) direct comparison of laser-induced damage threshold (LIDT) value change for HTA ceramic micro-optics has not been performed, however, increase in materials irradiation resiliency, compared to their polymer

counterparts,^[67,131] has been proposed^[132] and experimentally validated.^[133] Furthermore, LIDT of polymeric structures research results published so far, low material irreversible damage threshold is commonly attributed to organic compounds within the polymeric structures, with most significant being the use photo-initiator range.^[134] Organic compounds are associated with increased absorption in shorter UV–vis spectral regions. This can lead to a decrease in micro-optical component transmittance and LIDT values^[112] (Figure 3d). Similarly, effect of decrease of fabricated structure LIDT values, caused by the use of organic material, such as an epoxy-based SU-8, compared to the hybrid material, like SZ2080 and Ormo Clear, has been demonstrated by Zukauskas et al.^[135] Various optics and photonic areas would benefit from more laser radiation resilient micro-optical components. For instance, currently large interest is given to MPL fabricated refractive, diffractive or kinoform optical devices, such as binary phase Dammann diffractive optical element produced by^[136] for laser beam splitting applications or beam with desired angular orbital momentum (AOM) shape converter demonstrated.^[137] Calcination/pyrolysis is expected to further reduce limitations of MPL-based components and broaden their use in conjugation with high laser power systems. Heat treatment has also been shown to be a useful tool for manufacturing high-strength and structurally stable structures, making them ideal for use in micro-sized force sensors^[138] or scanning probe microscopes working in direct contact mode,^[139] where enhanced material strength could likely make components more stable when acted with force and extend life of the components. Additionally mechanically harder materials are preferred for master structure fabrication for soft lithography techniques, which also can be exploited via calcination/pyrolysis route.^[140]

Albiez et al. used the proprietary IP-Dip (Nanoscribe GmbH) resist and MPL process to make 3D pillars, and found that post-pyrolysis structures had Young's modulus as high as 47 GPa,^[141] which is on order higher than values reported for non heat-treated structures.^[142] Similarly, Bauer et al. were able to create silicon oxycarbide (SiOC) structures with Young's modulus of 66 GPa and the ability to withstand stresses up to 7 GPa.^[111] The ability to engineer material properties through techniques like heat treatment is critical for the extension of MPL technology into applications that require high structural resilience, such as high-power laser systems or astro-photonics and space, especially, if in the vacuum environment.

3.3. High Refractive Index Materials

When printing micro-optics, a high refractive index is commonly preferable, as in most cases it reduces the size of the refractive optical elements. It also adds capability of miniaturization for diffractive and free-form optical elements with a “faster” light bending. This requirement has become stronger recently, with the emergence of highly integrated optical systems, such as virtual reality optics or remotely controlled lightweight drones, for instance, as well as for space photonics. Where small size is critical, due to the size and weight of the VR goggles or the flying equipment. This has led to research activity into high-RI photopolymers suitable for mass-production techniques such as Nano-Imprint Lithography (NIL). The state of the art in NIL

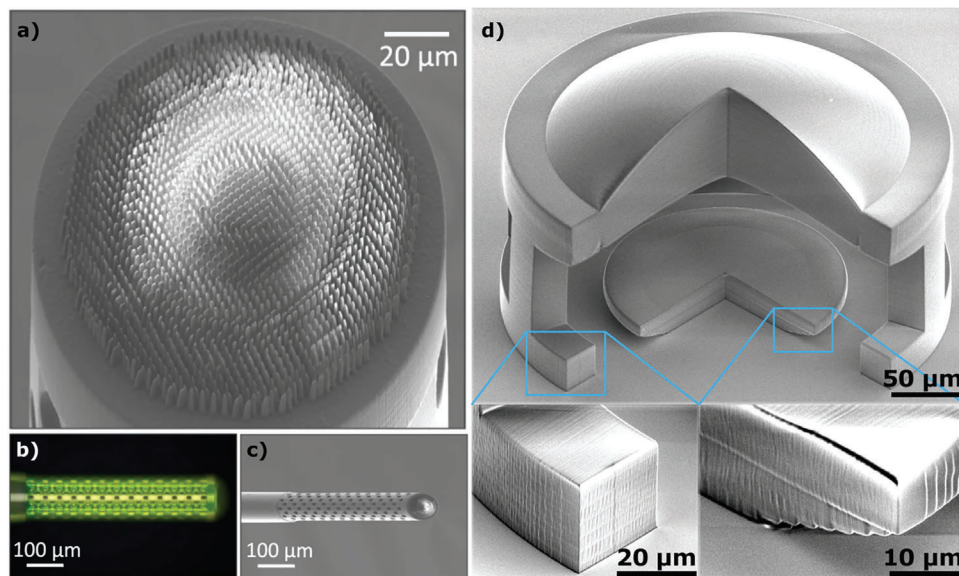


Figure 4. High precision pristine polymer structures for nanophotonics and microoptics which could have enhances performance if combined with HTA. a,c) SEM, b) optical images of the achromatic meta-fiber. Calcination could downscale it and increase its refractive index. Reproduced under the terms of the CC-BY license.^[148] Copyright 2022, Springer Nature. d) SEM image of an air-spaced doublet, which has been printed with one quarter cut out to better illustrate the internal structure. Pyrolysis could help in reduction of artifacts caused by non-uniform exposure during direct writing. Reproduced with permission.^[149] Copyright 2023, Optica Publishing Group.

photopolymers is $n = 1.90$ in visible range. This cannot be achieved with purely organic materials, whose refractive index in the visible range is in the order of 1.5.^[143,144] This shortcoming can be overcome by doping the photopolymer with nanoparticles, with the increase of RI to a maximum of 1.8^[144] (for 400–700 nm wavelength), however in this case, obtained organic–inorganic hybrid materials often suffer from high scattering and absorption losses and hindered structural resolution, which ultimately leads to insufficient quality micro-optical elements.^[145] Another notable micro-scale opto-element fabrication methods utilize multi-step sacrificial templating processes which broaden material selection but are complex and design-limiting.^[146,147]

Minimizing the listed offsetting factors and simplifying the manufacturing process have been proved through organic content removal, using the post-polymerization heat-treatment. A team led by Greer made high resolution TiO_2 photonic crystals using this technique.^[65] In this case, a Ti organic-inorganic hybrid was used, and an RI of 2.3 (for infrared wavelengths) was achieved. A team from Lyon used a different approach, doping a photopolymer with organically-ZrO₂ nanoparticles and then pyrolyzing the organic part.^[78] The RI achieved in this case was around 2.1 (400–800 nm). As it is evident from optical glass catalogs, optical elements of different refractive indices are required for compound optical setups and systems. Here, a new 3D miniaturization technique is emerging which can provide solutions via engineered pre-polymers for complex compound optical elements with optimized performance in imaging, spectroscopy and adaptable for integration with various established platforms. Additionally, an access to high refractive index materials, can further extend topic of meta-optics research offered by MPL offered 3D fabrication and integration options. As an example of which, recent achievements by Ren et al. (shown in **Figure 4a–c**, where

authors have demonstrated a wide bandwidth achromatic metalems working throughout the telecommunication range.^[148] In the case of metasurfaces, sufficient material's RI value is crucial to strongly confine light within structured geometries. In combination with controllable size reduction, HTA provides a way to increase overall component efficiency,^[50] while before inaccessible RI values can help to achieve sufficient phase delay modulation in shorter wavelength spectral range. Similarly high temperature treated MPL structures have attracted attention for use in the photonics field. As demonstrated by Liu et al.,^[87] where authors have achieved gyroid and woodpile photonic crystals with periods of 290 and 400 nm, respectively, isotropic material shrinkage and increase in optical density can be used to access UV–vis range while enhancing band-gap effects.

Another important aspect of HTA, regarding optical density of the material, is the observable RI value homogenization^[150] during annealing treatment. Refractive index of the material strongly depends on MPL process parameters, such as laser fluence, pulse repetition rate and wavelength values, including formed voxel overlapping during polymerization process.^[151] Besides that, RI can vary depending on the development procedure, accumulated internal stress or simply from aging.^[152] This effect, can ultimately may result in poor sample-to-sample repeatability as well as stability, and in the case of MPL fabrication processes utilizing grayscale/varying laser exposure parameters for voxel dimensions control,^[153] can lead to unaccounted RI modulation throughout the formed element. In the case of imaging systems formed though grayscale MPL, as the one demonstrated by Siegle et al.^[149] (**Figure 4d**), uncertainty of index of refraction of the material may introduce additional optical aberrations, that are extremely hard to correct, due to the lack of volumetric RI metrology systems for micro-/nano-scale objects. Thus as an added benefit, the HTA initiated thermal polymer cross-linking acts as a

post-bake procedure,^[152] alleviating the uncertainty of material properties (*“exposure memory”* caused by specific direct write strategy) and increase repeatability of functional micro-optical systems.

3.4. Optically Active Compounds

The use of MPL has gathered significant attention in the modification of photo-active materials due to its ability to create intricate 3D devices in the micrometre size range. These structures have potential use cases in a variety of fields, including chip-scale photonic communication systems, bioimaging, and microlasers. The incorporation of photo-activators allows for the tunability of not only mechanical and chemical characteristics, but also optical material properties.

However, traditional resists often contain mixtures of organic compounds with complex molecular compositions that limit the use of MPL-structured materials as photonic devices. The organic resist fraction can lead to increased absorption and poor chemical and thermal stability, as well as a relatively low LIDT that prohibits the use of the material with high-power light excitation.^[66] Nevertheless, use of organic dyes as dopants in MPL-formed structures has been reported numerous times, for active micro-photonic devices. However, these materials can have large absorption cross-sections and broad emissions, leading to high lasing thresholds and low thermal and chemical stability,^[154] also suffering from rapid photo-bleaching of organic molecules in ambient conditions.^[155]

Glass host material is more desirable, and is routinely doped with active ions such as Neodymium, Erbium, Ytterbium, and Europium, to make the active material for solid-state lasers.^[156] Inorganic materials have high lattice-binding energy, making them useful for decreasing non-radiative relaxation processes and increasing stability. A similar result can be achieved by the pyrolysis/calcination of an organic-inorganic hybrid materials doped with such active ions. There have been several publications on heat-treated MPL-formed photo-active structures, with a common focus on lanthanide-doped materials due to their strong emission in the visible and near-infrared range and their ability to retain their optical properties, like emission spectrum bandwidth regardless of the surrounding host material, thanks to the shielding of the 4f orbitals by the 5s² and 5p⁶ shells. Active 3D structures fabricated by this method were first demonstrated by Wen et al.,^[66] where they fabricated micro-toroid optical resonators can reach quality factors Q of over 10⁴. Additionally, unprecedentedly high resistance to laser-induced damage has been reached. Cooperstein et al. reported laser fluence values of excitation source as high as 1.87 J cm⁻² without any noticeable damage to the manufactured light splitter structures made from yttrium aluminum garnet ceramics doped with neodymium.^[67]

In the case of resonator structures, MPL is already proven to be competitive and routinely used alternative to other manufacturing methods, due to its rapid prototyping capabilities, geometrical flexibility and ease of processing.^[157] For instance, Zhang et al. demonstrated the feasibility of highly complex integrated optical sensing systems using MPL.^[55] Additionally, the expanded choice of transparent inorganic materials that can be doped with active ions without compromising the possible geometry com-

plexity is expected to further strengthen the role of MPL in the formation of optical resonators and the development of complex systems. In the field of optical measurement systems, the use of new optically active materials can help to reduce the signal-to-noise ratio,^[158] eliminate oxygen quenching effects affecting organic compounds, the excellent thermal and chemical stability of these materials can expand the application areas of such sensors, leading to further improvements in the achievements demonstrated so far.

With the emergence of new efforts on heat treated optically active structures, several common issues have been observed, such as porosity (due to polycrystalline structure) caused scattering losses and emission quenching due to activator clustering. However, these issues can be minimized through the use of matrix composition substitution, as demonstrated by Winczewski et al. with 3D luminescent silicon-free ZrO₂:Eu³⁺ nanostructures.^[85] These recent developments provide a new platform for the future development of 3D luminescent and active devices.

3.5. Complex Systems

Current widely used methods for glass phase micro-optics, for example, precision press glass moulding, grinding or polishing, lack flexibility for one-off prototypes or more complex multi-element optic assemblies. Whereas the importance of the results achieved by thermal treatment, brought freedom of choice of material properties and MPL, nano-scale precision combination are visible in the examples of the complex micro-scale multi-element optical systems.^[2] Additive MPL method's strength of fabricating complex systems, without the need of component alignment,^[3] is maintained, due to the isotropic material shrinkage during heat treatment process, as long as structure is not limited mechanically. Common exception and geometrical deformation source being material that is adhered to the substrate. In order to decrease deformation due to the adhesion forces between substrate and structured material, a common choice is to create an additional supporting structures.^[89] These elements act as an intermediate link between the primary structure and a substrate reducing structural defects arising from the coupling between the two. With the example of pre-designed structures, most of the material anisotropic deformation can be pre-compensated by introducing shrinkage-guides at specific angles.^[131]

Interestingly, the material shrinkage can be exploited advantageously by utilizing the material's adhesion to the substrate points and applying designed pre-compensation sacrificial support structures. For instance, incorporation of hinge systems, similarly to the already discussed micro-sized force sensors developed by Power et al.^[138] (Figure 5b), a pre-designed non-isotropic material deformation may be achieved. Such a tool could be used for evanescent wave coupling/decoupling cases, where a nanometer gap between separate optical elements are needed and are currently very hard to obtain directly via MPL due to the cross-linked material proximity effects^[160,161] and dark reaction polymerization.^[162] Ability to create extremely fine and accurate (<200 nm) structures in a highly reproducible manner is currently inaccessible to traditional MPL. Yet it is highly desired in applications for micro-lasers^[163] and coherent quantum photonics,^[159,164] an example given in Figure 5c. Another

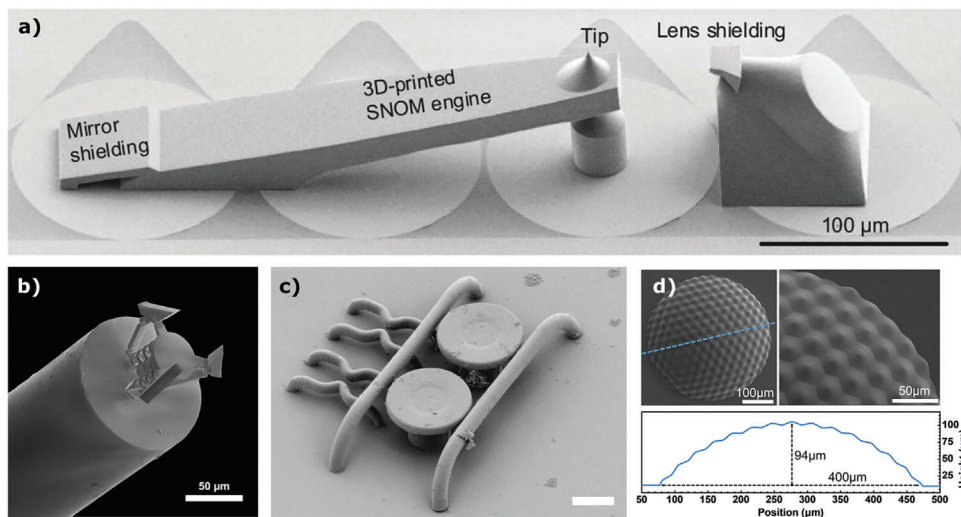


Figure 5. Intricate design capabilities realized with MPL technology. a) SEM image of the Scanning-probe microscopy engine. Reproduced under the terms of the CC-BY-NC-ND license.^[53] Copyright 2019, WILEY-VCH. b) SEM image of the gripper-tipped optical fiber. Reproduced with permission.^[138] Copyright 2018, John Wiley and Sons. c) SEM image of 3D quantum optical assembly of micro-resonators, waveguides and couplers. Reproduced under the terms of the CC-BY-NC license.^[159] Copyright 2013, Nature Publishing. d) Morphologies of the as-prepared logarithmic, top images are overall and magnified SEM images, and the bottom results are relative cross-section profiles. Reproduced under the terms of the CC-BY license.^[3] Copyright 2022, Springer Nature. All of the structures would benefit by HTA due to increased optical transparency and mechanical rigidity (a), stability and durability (b), precise arrangement (c), material homogenization (d), respectively.

significant factor linked to multi-element optical systems are accumulative losses due to the multiple Fresnel reflections. With increasing number of optical interfaces, losses can quickly accumulate and reach non-negligible levels. For instance, in the case of three lens objective system, six interfaces correspond 20% transmission losses, for material with refractive index value of 1.5.^[119] Recently, Ristok et al.^[165] has demonstrated a viable option of significantly reducing reflection losses. Authors demonstrated that structures formed through MPL can be further be processed using Atomic Layer Deposition (ALD) coating method for high efficiency anti-reflective coatings, minimizing reflection losses down to 1 % levels. However, in the published study, authors have observed coated micro-optical component degradation and formation of defects attributed to the coating process. Even in the case of low processing temperature (150 °C^[165]) ALD systems coated samples are exposed to the rise of ambient temperature and low pressures, as well as internal force accumulation due to the mismatch of sample and coating material thermal expansion coefficients. All of which can cause sample swelling, fractures and film delamination. Heat treated ceramic structures, have been proven to be more stable in the case of high or low temperature,^[86] furthermore, presence of internal stresses between coated material and the structure is expected to be decreased due to the better thermal expansion matching between the inorganic materials.^[166] Thus, HTA can act as an additional step for further technological improvement for compound micro-optical components.

Additionally, calcination helps in broadening the selection of resulting structurable materials, which can further improve compound optical micro systems. Up till now the selection for highly absorbing polymerizable materials has been practically non-existent, with the notable exception of recently demonstrated Prototype IP-Black (Nanoscribe GmbH Co. KG)

photoresist.^[167] Opaque micro elements had to be created via additional and complex steps as highly absorbing ink incorporation into printed structures^[168] or using non-transparent film coating techniques.^[169] Efficient absorber materials like SiOC-based ceramics have been proven to possess high absorption in visible and longer wavelength ranges^[170] and could be used for directly printable aperture elements, needed to achieve imaging systems of the highest quality by reducing aberrations, as vignetting and attenuation of background stray light. SiOC ceramics are also ensuring the superb mechanical properties exceeding all the other 3D printed substances.^[140]

The versatility of heat-treated materials makes them suitable for opto-mechanical systems, as the ones demonstrated by Dietrich et al.^[53] (Figure 5a). Specifically, for in direct contact mode operating atomic force microscopy systems, which require materials that are mechanically robust to withstand harsh conditions and repeated use, as well as transparent to enable the use of optical sensing. Calcination improves both of these aspects, making it beneficial for such systems.

Combination of MPL and thermal treatment becomes a powerful tool for creating complex, high durability and stability with fully 3D freedom of form, micro-optical components and nanostructures. However, in order to attract any significant relevance in industry, reliable methods scaling up of manufacture throughput have to be realized. This problem is particularly important in the case of HTA, due to the additional geometry shrinkage and mass loss during annealing post-process. Conventional parallelization techniques, as usage of multiple laser beams through using micro lens arrays, DOEs or simple beam splitter setups are not prohibited and can be used. Possibility of using process sequencing by breaking down the manufacturing process into a series of optimized and most appropriate technology steps has been demonstrated

by Schmidt et al. in their proof of concept study.^[171] Authors have successfully achieved combination of two different scale lithography technologies, DLP- structuring of material in the typical scale of tenths of microns to centimeters in dimension, and MPL. Demonstration of substrate-free mm range woodpile structures with additionally structured lattices with individual feature sizes of approximately 1 μm with no observed deformation of both scale objects after HTA at 1000 °C is a promising result for complex optical system. Hybridization of several technologies allows the production of large scale compound systems while maintaining sub-wavelength precision in the fictionalized structures, such as biochip systems with integrated polymeric filtering structures demonstrated by Wu et al.^[172] Meanwhile Hu et al.^[3] showcased compound lens systems, illustrated in Figure 5d. The second example provides an excellent demonstration of the potential benefits of hybridization diverse lithography techniques, where the most part of the bulk components can be produced using larger scale additive manufacturing methods like UV irradiation based SLA or DLP. Whereas, the micro-lens structures that require higher precision can be manufactured through MPL employing ultrafast laser. By combining both of these methods, it becomes feasible to create integrated multi-scale systems of various dimensions. We foresee the calcination to give advantage by merging these two-exposure steps made structures homogenizing into a monolith object without leaving boundary traces if the same or similar materials are used.

3.6. Challenges

Despite numerous advantages are being brought by calcination combining it with MPL technique, yet some challenges are raising concern of being met in the development way. One of the key challenges in using MPL-fabricated and heat-treated structures as micro-optical components is the precise control of the calcination process itself. As explained, the heat treatment at elevated temperatures exceeding 1000 °C is necessary to convert the organic material into a pure inorganic structure, but it can also hypothetically lead to structural changes, such as shrinkage and cracking, that can degrade the optical properties of the micro-optics. The control of these effects is essential to maintain the desired optical performance, such as low scattering and high transmission, and requires careful selection of calcination parameters such as temperature, heating rate, duration, and atmosphere or even the applied substrate. One of frequently encountered difficulties arising from heating the material at high temperatures is the formation of free carbon, but there can be more which are not met yet.

The most expected obstacles for a versatile calcination route are:

- Free carbon formation - which can darken the substance and reduce its transparency;
- Cracks (fissure) - larger volume or scale work-pieces can start cracking reaching some dimensions or being attached to the substrate of different expansion;
- Porosity - evaporation of organic matter and application of gases can cause pore formation in the surfaces or also in the volume;
- Polycrystalline domain evolution. Arising from HTA material phase conversion, polycrystalline domain induced light scattering.
- Deformation - loss of defined structural integrity;
- Lack of simulation tools for structural changes, caused by HTA at micro-/nano-scales;
- Limited volumetric metrology tools with nano-scale precision for a proper characterization.

However, the mentioned concerns have not yet prohibited the emergence of successful MPL-HTA combination for 3D micro-optics. They are still not seen as hard obstacles due to their non-fundamental, yet rather technological type, which in turn can be solved using various techniques perfected in advanced material processing, nano-lithography, self-assembly, and other industrially mature fields.

4. Summary and Trends for the Future

Here, we summarize and foresee important near future aspects emerging as a new branch of additive manufacturing by combining ultrafast laser lithography with high-temperature annealing. It empowers 3D printing of glass/ceramics with uncompromising spatial resolution, production throughput, and flexibility.

- Heat treatment as a post-process for MPL manufactured structures broadens selection of key material parameters, such as RI, chemical/thermal stability and LIDT. Adaption of newly reachable capabilities and expansion of use cases in micro-optics and photonics is expected to follow. With further experimental approaches either through post processing solutions or chemical engineering, it is likely that advances in these areas will continue to drive the development of improved micro-optics structures with a wider range of functionalities in photo-active sensors, telecommunications, micro-chip devices and high power laser micro-optics. Calcination and pyrolysis are useful tools in certain circumstances, but their reliance on high temperatures imposes strict restrictions on material selection. This contrasts with the general assertion that micro-patterning lithography (MPL) is a key link between various manufacturing technologies. Additional attention to manufactured micro-scale structure handling and transportation will be needed, but can be solved via technological means.
- The challenge is foreseen for production of larger-scale complex-shaped optical elements and multi-material components, though not restricted by fundamental limits, rather technological solutions. One can anticipate incorporation of MPL+ calcination in macro optic components and robust metrology techniques.
- MPL combined with calcination empowers additive manufacturing of high-resolution inorganic 3D micro-/nano-optical structures employing established and commercially available laser lithography setups without the need of their cumbersome rearrangement (as for STED) or significant upgrading (as for laser direct sintering).

Apart of relevance to photonics, lasers and broader scope of light technologies described above, the volumetric hot-pot

glass making is becoming a large surface-to-volume technique conducive to efficient chemical reactions occurring across the interface during the pyrolysis/calcination/sintering step. Glass transition governed by thermodynamics and kinetics can use the emerging 3D printing and high temperature treatments as a test bed for glass formation research, which never had access to small volumes, fast chemical reactions, high doping gradients, and thermal quenching. Glasses are unlimited to the types of chemical bonding and can continue to pave technological progress in this century of Light.

Acknowledgements

This research received funding from the EU Horizon 2020, Research and Innovation program LASERLAB-EUROPE JRA project no. 871124 (M.F., G.B., and M.M.).

Open access publishing facilitated by Swinburne University of Technology, as part of the Wiley - Swinburne University of Technology agreement via the Council of Australian University Librarians.

Conflict of Interest

The authors declare no conflict of interest.

Keywords

3D printing, additive manufacturing, advanced materials, calcination, laser direct writing, micro-optics, post-processing

Received: December 31, 2022

Revised: April 8, 2023

Published online: May 14, 2023

- [1] E. Skliutas, M. Lebedevaite, E. Kabouraki, T. Baldacchini, J. Ostrauskaite, M. Vamvakaki, M. Farsari, S. Juodkazis, M. Malinauskas, *Nanophotonics* **2021**, *10*, 12111.
- [2] Z. Hong, P. Ye, D. A. Loy, R. Liang, *Adv. Sci.* **2022**, *9*, 2105595.
- [3] Z.-Y. Hu, Y.-L. Zhang, C. Pan, J.-Y. Dou, Z.-Z. Li, Z.-N. Tian, J.-W. Mao, Q.-D. Chen, H.-B. Sun, *Nat. Commun.* **2022**, *13*, 1.
- [4] D. Gonzalez-Hernandez, S. Varapnickas, A. Bertocini, C. Liberale, M. Malinauskas, *Adv. Opt. Matter.* **2023**, *11*, 2201701.
- [5] J. Sun, D. Ye, J. Zou, X. Chen, Y. Wang, J. Yuan, H. Liang, H. Qu, J. Binner, J. Bai, *J. Mater. Sci. Technol.* **2022**, *138*, 1.
- [6] Z. Chen, Z. Li, J. Li, C. Liu, C. Lao, Y. Fu, C. Liu, Y. Li, P. Wang, Y. He, *J. Eur. Ceram. Soc.* **2019**, *39*, 661.
- [7] I. Karakurt, L. Lin, *Curr. Opin. Chem. Eng.* **2020**, *28*, 134.
- [8] G. Zhang, B. Zou, X. Wang, Y. Yu, Q. Chen, *Ceram. Int.* **2023**, *49*, 1009.
- [9] J. Šafka, M. Seidl, I. Kovalenko, L. Voleský, M. Ackermann, V. Truxová, *MM Sci. J.* **2020**, *2020*, 3905.
- [10] R. Gmeiner, G. Mitteramskogler, J. Stampfl, A. R. Boccaccini, *Int. J. Appl. Ceram. Technol.* **2015**, *12*, 38.
- [11] Y. Ye, Y. Du, T. Hu, J. You, B. Bao, Y. Wang, T. Wang, *Ind. Eng. Chem. Res.* **2021**, *60*, 9368.
- [12] M. Schwentenwein, J. Homa, *Int. J. Appl. Ceram. Technol.* **2015**, *12*, 1.
- [13] H. Elsayed, P. Colombo, E. Bernardo, *J. Eur. Ceram. Soc.* **2017**, *37*, 4187.
- [14] K. A. Seerden, N. Reis, J. R. Evans, P. S. Grant, J. W. Halloran, B. Derby, *J. Am. Ceram. Soc.* **2001**, *84*, 2514.
- [15] A. Bhatti, M. Mott, J. Evans, M. Edirisinghe, *J. Mater. Sci. Lett.* **2001**, *20*, 1245.
- [16] H. Masuda, Y. Ohta, M. Kitayama, *J. Mater. Sci. Chem. Eng.* **2019**, *7*, 1.
- [17] N. M. Pu'ad, R. A. Haq, H. M. Noh, H. Abdullah, M. Idris, T. Lee, *Mater. Today Proc.* **2020**, *29*, 228.
- [18] C. L. Cramer, A. M. Elliott, E. Lara-Curzio, A. Flores-Betancourt, M. J. Lance, L. Han, J. Blacker, A. A. Trofimov, H. Wang, E. Cakmak, K. Nawaz, *J. Am. Ceram. Soc.* **2021**, *104*, 5467.
- [19] C. Griffin, J. Daufenbach, S. McMillin, in *1994 International Solid Freeform Fabrication Symposium*, The University of Texas, Austin, Texas, **1994**.
- [20] B. Duan, M. Wang, *J. R. Soc. Interface* **2010**, *7*, S615.
- [21] J. S. Yun, T.-W. Park, Y. H. Jeong, J. H. Cho, *Appl. Phys. A* **2016**, *122*, 1.
- [22] N. Kovacev, S. Li, K. Essa, *J. Eur. Ceram. Soc.* **2021**, *41*, 7734.
- [23] M. Lejeune, T. Chartier, C. Dossou-Yovo, R. Noguera, *J. Eur. Ceram. Soc.* **2009**, *29*, 905.
- [24] A. Sotov, A. Kanyukov, A. Popovich, V. Sufiarov, *Ceram. Int.* **2021**, *47*, 30358.
- [25] E. Özkol, A. M. Wätjen, R. Bermejo, M. Deluca, J. Ebert, R. Danzer, R. Telle, *J. Eur. Ceram. Soc.* **2010**, *30*, 3145.
- [26] O. Santoliquido, F. Camerota, A. Ortona, *Open Ceram.* **2021**, *5*, 100059.
- [27] R. Zhou, Y. Wang, Z. Liu, Y. Pang, J. Chen, J. Kong, *Nano-Micro Lett.* **2022**, *14*, 122.
- [28] R. Bahr, X. He, B. Tehrani, M. M. Tentzeris, in *2018 IEEE/MTT-S Int. Microwave Symp.-IMS*, IEEE, **2018**, pp. 1561–1564.
- [29] W. Jung, Y.-H. Jung, P. V. Pikhitsa, J. Feng, Y. Yang, M. Kim, H.-Y. Tsai, T. Tanaka, J. Shin, K.-Y. Kim, H. Choi, J. Rho, M. Choi, *Nature* **2021**, *592*, 54.
- [30] W. Hegge, D. Bohling, J. Chou, M. McAllister, P. Schottland, in *SID Symposium Digest of Technical Papers*, vol. 42. Wiley, Hoboken, NJ, **2011**, pp. 837–840.
- [31] A. G. Mark, J. G. Gibbs, T.-C. Lee, P. Fischer, *Nat. Mater.* **2013**, *12*, 802.
- [32] M. Richard, A. Al-Ajaji, S. Ren, A. Foti, J. Tran, M. Frigoli, B. Gusarov, Y. Bonnassieux, E. G. Caurel, P. Bulkin, R. Ossikovski, A. Yassar, *Adv. Colloid Interface Sci.* **2020**, *275*, 102080.
- [33] A. Berg, H. Jonkman, K. Loos, G. Portale, B. Noheda, *ACS Appl. Nano Mater.* **2022**, *5*, 13349.
- [34] W. Kim, G. Yoon, J. Kim, H. Jeong, Y. Kim, H. Choi, T. Badloe, J. Rho, H. Lee, *Microsyst. Nanoeng.* **2022**, *8*, 73.
- [35] G. Yoon, K. Kim, S.-U. Kim, S. Han, H. Lee, J. Rho, *ACS Nano* **2021**, *15*, 698.
- [36] J. Kim, D. K. Oh, H. Kim, G. Yoon, C. Jung, J. Kim, T. Badloe, H. Kang, S. Kim, Y. Yang, J. Lee, B. Ko, J. G. Ok, J. Rho, *Laser Photonics Rev.* **2022**, *16*, 2200098.
- [37] L. Keller, M. Huth, *Beilstein J. Nanotechnol.* **2018**, *9*, 2581.
- [38] H. Plank, C. Gspan, M. Dienstleder, G. Kothleitner, F. Hofer, *Nanotechnology* **2008**, *19*, 485302.
- [39] T. Reitberger, J. Franke, G.-A. Hoffmann, L. Overmeyer, L. Lorenz, K.-J. Wolter, in *2016 12th Int. Congress Molded Interconnect Devices (MID)*, IEEE, **2016**, pp. 1–6.
- [40] W.-G. Kim, J.-M. Lee, Y. Yang, H. Kim, V. Devaraj, M. Kim, H. Jeong, E.-J. Choi, J. Yang, Y. Jang, T. Badloe, D. Lee, J. Rho, J. T. Kim, J.-W. Oh, *Nano Lett.* **2022**, *22*, 4702.
- [41] S. Behera, J. Joseph, *Opt. Lett.* **2017**, *42*, 2607.
- [42] Y.-J. Jen, J.-W. Huang, W.-C. Liu, S. Chan, C.-H. Tseng, *Opt. Mater. Express* **2016**, *6*, 697.
- [43] S. Sarkar, K. Samanta, J. Joseph, *Opt. Express* **2020**, *28*, 4347.

- [44] U. Kilic, M. Hilfiker, A. Ruder, R. Feder, E. Schubert, M. Schubert, C. Argyropoulos, *Adv. Funct. Mater.* **2021**, *31*, 2010329.
- [45] L. Jonušauskas, D. Gailevičius, S. Rekštytė, T. Baldacchini, S. Juodkazis, M. Malinauskas, *Opt. Express* **2019**, *27*, 15205.
- [46] V. Hahn, P. Kiefer, T. Frenzel, J. Qu, E. Blasco, C. Barner-Kowollik, M. Wegener, *Adv. Funct. Mater.* **2020**, *30*, 1907795.
- [47] G. I. Greisukh, E. G. Ezhov, A. L. Il'ya, S. A. Stepanov, *Appl. Opt.* **2010**, *49*, 4379.
- [48] D. Malacara-Hernández, Z. Malacara-Hernández, *Handbook of Optical Design*, CRC Press, Boca Raton, FL, **2017**.
- [49] A. Y. Zhu, W. T. Chen, A. Zaidi, Y.-W. Huang, M. Khorasaninejad, V. Sanjeev, C.-W. Qiu, F. Capasso, *Light Sci. Appl.* **2018**, *7*, 17158.
- [50] W. T. Chen, A. Y. Zhu, F. Capasso, *Nat. Rev. Mater.* **2020**, *5*, 604.
- [51] T. Zhan, J. Xiong, Y.-H. Lee, S.-T. Wu, *Opt. Express* **2018**, *26*, 35026.
- [52] Z. Lin, V. Liu, R. Pestourie, S. G. Johnson, *Opt. Express* **2019**, *27*, 15765.
- [53] P.-I. Dietrich, G. Göring, M. Trappen, M. Blaicher, W. Freude, T. Schimmel, H. Hölscher, C. Koos, *Small* **2020**, *16*, 1904695.
- [54] D. Gonzalez-Hernandez, S. Varapnickas, A. Bertocchini, C. Liberale, M. Malinauskas, *Adv. Opt. Mater.* **2023**, *11*, 2201701.
- [55] S. Zhang, S.-J. Tang, S. Feng, Y.-F. Xiao, W. Cui, X. Wang, W. Sun, J. Ye, P. Han, X. Zhang, Y. Zhang, *Adv. Opt. Mater.* **2019**, *7*, 1900602.
- [56] T. Gissibl, S. Thiele, A. Herkommer, H. Giessen, *Nat. Photonics* **2016**, *10*, 554.
- [57] S. Schizas, V. Melissinaki, A. Gaidukeviciute, C. Reinhardt, C. Ohrt, V. Dedoussis, B. N. Chichkov, C. Fotakis, M. Farsari, D. Karalekas, *Int. J. Adv. Manuf. Technol.* **2010**, *48*, 435.
- [58] H. Xia, J. Wang, Y. Tian, Q.-D. Chen, X.-B. Du, Y.-L. Zhang, Y. He, H.-B. Sun, *Adv. Mater.* **2010**, *22*, 3204.
- [59] F. Jin, J. Liu, Y.-Y. Zhao, X.-Z. Dong, M.-L. Zheng, X.-M. Duan, *Nat. Commun.* **2022**, *13*, 1.
- [60] S. Juodkazis, *Opto-Electron. Adv.* **2023**, *6*, 230023.
- [61] S. Fu, M. Zhu, Y. Zhu, *J. Adv. Ceram.* **2019**, *8*, 457.
- [62] F. Ainger, J. Herbert, *Special Ceram.* **1960**, *168*, 81.
- [63] P. Colombo, G. Mera, R. Riedel, G. D. Soraru, *Ceram. Sci. Technol.* **2013**, *245*.
- [64] G. Seniutinas, A. Weber, C. Padeste, I. Sakellari, M. Farsari, C. David, *Microelectron. Eng.* **2018**, *191*, 25.
- [65] A. Vyatskikh, R. C. Ng, B. Edwards, R. M. Briggs, J. R. Greer, *Nano Lett.* **2020**, *20*, 3513.
- [66] X. Wen, B. Zhang, W. Wang, F. Ye, S. Yue, H. Guo, G. Gao, Y. Zhao, Q. Fang, C. Nguyen, X. Zhang, J. Bao, J. T. Robinson, P. M. Ajayan, J. Lou, *Nat. Mater.* **2021**, *20*, 1506.
- [67] I. Cooperstein, S. C. Indukuri, A. Bouketov, U. Levy, S. Magdassi, *Adv. Mater.* **2020**, *32*, 2001675.
- [68] C. Greant, B. V. Durme, J. V. Hoorick, S. V. Vlierberghe, *Adv. Funct. Mater.* **2023**, 2212641 <https://doi.org/10.1002/adfm.202212641>
- [69] T. A. Pham, D.-P. Kim, T.-W. Lim, S.-H. Park, D.-Y. Yang, K.-S. Lee, *Adv. Funct. Mater.* **2006**, *16*, 1235.
- [70] F. Kotz, K. Plewa, W. Bauer, N. Schneider, N. Keller, T. Nargang, D. Helmer, K. Sachsenheimer, M. Schäfer, M. Worgull, C. Greiner, C. Richter, B. E. Rapp, *Adv. Mater.* **2016**, *28*, 4646.
- [71] F. Kotz, A. S. Quick, P. Risch, T. Martin, T. Hoose, M. Thiel, D. Helmer, B. E. Rapp, *Adv. Mater.* **2021**, *33*, 2006341.
- [72] P.-I. Dietrich, M. Blaicher, I. Reuter, M. Billah, T. Hoose, A. Hofmann, C. Caer, R. Dangel, B. Offrein, U. Troppenz, M. Moehle, W. Freude, C. Koos, *Nat. Photonics* **2018**, *12*, 241.
- [73] M. Schumann, T. Bückmann, N. Gruhler, M. Wegener, W. Pernice, *Light Sci. Appl.* **2014**, *3*, e175.
- [74] J.-W. Yeh, Y.-L. Chen, S.-J. Lin, S.-K. Chen, *Mater. Sci. Forum.* **2007**, *560*, 1.
- [75] J.-W. Yeh, S.-K. Chen, S.-J. Lin, J.-Y. Gan, T.-S. Chin, T.-T. Shun, C.-H. Tsau, S.-Y. Chang, *Adv. Eng. Mat.* **2004**, *6*, 299.
- [76] J. Köpfler, T. Frenzel, J. Schmalian, M. Wegener, *Adv. Mater.* **2021**, *33*, 2103205.
- [77] F. Kotz, P. Risch, K. Arnold, S. Sevim, J. Puigmartí-Luis, A. Quick, M. Thiel, A. Hrynevich, P. D. Dalton, D. Helmer, B. E. Rapp, *Nat. Commun.* **2019**, *10*, 1.
- [78] A. Desponds, A. Banyasz, D. Chateau, A. Tellal, A. Venier, S. Meille, G. Montagnac, J. Chevalier, C. Andraud, P. L. Baldeck, S. Parola, *Small* **2021**, *17*, 2102486.
- [79] A. Desponds, A. Banyasz, G. Montagnac, C. Andraud, P. Baldeck, S. Parola, *Solgel Sci. Technol.* **2020**, *95*, 733.
- [80] M. Malinauskas, A. Žukauskas, G. Bičkauskaitė, R. Gadonas, S. Juodkazis, *Opt. Express* **2010**, *18*, 10209.
- [81] G. Merkininkaitė, E. Aleksandravičius, S. Varapnickas, D. Gailevičius, S. Šakirzanovas, M. Malinauskas, *Ultrafast Laser Nanostructuring, Springer Series in Optical Sciences* **2023**, *239*, 787.
- [82] D. Gailevičius, V. Padolskytė, L. Mikoliūnaitė, S. Šakirzanovas, S. Juodkazis, M. Malinauskas, *Nanoscale Horiz.* **2019**, *4*, 647.
- [83] L. Jonušauskas, D. Gailevičius, L. Mikoliūnaitė, D. Sakalauskas, S. Šakirzanovas, S. Juodkazis, M. Malinauskas, *Materials* **2017**, *10*, 12.
- [84] L. Yang, F. Mayer, U. H. Bunz, E. Blasco, M. Wegener, *Light: Adv. Manuf.* **2021**, *2*, 296.
- [85] J. Winczewski, M. Herrera, C. Gabriel, I. Izeddin, S. Gabel, B. Merle, A. Susarrey Arce, H. Gardeniers, *Adv. Opt. Mater.* **2022**, *2102758*.
- [86] G. Merkininkaitė, E. Aleksandravičius, M. Malinauskas, D. Gailevičius, S. Šakirzanovas, *Opt.-Electron. Adv.* **2022**, *5*, 1.
- [87] Y. Liu, H. Wang, J. Ho, R. C. Ng, R. J. Ng, V. H. Hall-Chen, E. H. Koay, Z. Dong, H. Liu, C.-W. Qiu, J. R. Greer, K. W. Yang, *Nat. Commun.* **2019**, *10*, 1.
- [88] T. Doualle, J.-C. André, L. Gallais, *Opt. Lett.* **2021**, *46*, 364.
- [89] Z. Vangelatos, L. Wang, C. P. Grigoropoulos, *J. Micromech. Microeng* **2020**, *30*, 055008.
- [90] E. Bernardo, L. Fiocco, G. Parcianello, E. Storti, P. Colombo, *Materials* **2014**, *7*, 1927.
- [91] S. Ishihara, H. Gu, J. Bill, F. Aldinger, F. Wakai, *J. Am. Ceram. Soc.* **2002**, *85*, 1706.
- [92] L.-A. Liew, R. Saravanan, V. M. Bright, M. L. Dunn, J. W. Daily, R. Raj, *Sens. Actuators, A* **2003**, *103*, 171.
- [93] S. Tsukuda, S. Seki, S. Tagawa, M. Sugimoto, A. Idesaki, S. Tanaka, A. Oshima, *J. Phys. Chem. B* **2004**, *108*, 3407.
- [94] S. Srivastava, D. Avasthi, J. Pivin, *Nucl. Instrum. Methods Phys. Res., Sect. B* **2002**, *191*, 718.
- [95] G. Chandra, T. E. Martin, Rapid thermal process for obtaining silica coatings, **1991**, US Patent 5,059,448.
- [96] P. Colombo, A. Martucci, O. Fogato, P. Villorosi, *J. Am. Ceram. Soc.* **2001**, *84*, 224.
- [97] J. Wilden, G. Fischer, *Appl. Surf. Sci.* **2007**, *254*, 1067.
- [98] J. Mukherjee, A. Ranjan, A. Saxena, P. K. Das, R. Banerjee, *Appl. Surf. Sci.* **2013**, *270*, 219.
- [99] E. Bouyer, G. Schiller, M. Müller, R. Henne, *Plasma Chem. Plasma Process.* **2001**, *21*, 523.
- [100] C. Kim, I.-B. Sohn, Y. J. Lee, C. C. Byeon, S. Y. Kim, H. Park, H. Lee, *Opt. Mater. Express* **2014**, *4*, 2233.
- [101] C. E. Soteropoulos, K. M. Zurick, M. T. Bernards, H. K. Hunt, *Langmuir* **2012**, *28*, 15743.
- [102] T. E. Dimmick, G. Kakarantzas, T. A. Birks, P. S. J. Russell, *Appl. Opt.* **1999**, *38*, 6845.
- [103] Z.-Z. Li, L. Wang, H. Fan, Y.-H. Yu, Q.-D. Chen, S. Juodkazis, H.-B. Sun, *Light: Sci. Appl.* **2020**, *9*, 41.
- [104] A. Rudenko, J.-P. Colombier, S. Höhm, A. Rosenfeld, J. Krüger, J. Bonse, T. Itina, *Sci. Rep.* **2017**, *7*, 12306.
- [105] B. Wu, H. Zhu, B. Zhang, F. Ren, S. Juodkazis, F. Chen, *Mater. Today Nano* **2022**, *21*, 100299.

- [106] A. Žukauskas, M. Malinauskas, G. Seniutinas, S. Juodkakis, *Rapid Laser Optical-Printing in 3D at a Nanoscale*, Ch. 1, Wiley, Hoboken, NJ, **2016**.
- [107] S. Ng, S. Juodkakis, Nanoscale Plasmonic Printing. in *Ultrafast Laser Nanostructuring: The Pursuit of Extreme Scales* (Eds. R. Stoian and J. Bonse), Vol. 239, Ch. 25, Springer, Berlin, **2023**.
- [108] E. G. Gamaly, A. V. Rodde, *Appl. Phys. A* **2018**, *124*, 1.
- [109] C. Mack, *Optical Lithography, field guides*, SPIE, Paris **2006**.
- [110] C. Kerse, H. Kalaycıoğlu, P. Elahi, B. Çetin, D. Kesim, O. Akçaalan, S. Yavaş, M. Aşik, B. Öktem, H. Hoogland, R. Holzwarth, F. Ilday, *Nature* **2016**, *537*, 84.
- [111] J. Bauer, C. Crook, A. G. Izard, Z. C. Eckel, N. Ruvalcaba, T. A. Schaedler, L. Valdevit, *Matter* **2019**, *1*, 1547.
- [112] A. Žukauskas, G. Batavičiūtė, M. Ščiuka, Z. Balevičius, A. Melninkaitis, M. Malinauskas, *Opt. Mater. Express* **2015**, *39*, 224.
- [113] Z. Hong, P. Ye, D. A. Loy, R. Liang, *Optica* **2021**, *8*, 904.
- [114] F. Sala, P. Paié, R. Martínez Vázquez, R. Osellame, F. Bragheri, *Micromachines* **2021**, *12*, 180.
- [115] C.-H. Lin, L. Jiang, Y. Chai, H. Xiao, S.-J. Chen, H. Tsai, *Appl. Phys. A* **2009**, *97*, 751.
- [116] F. Han, S. Gu, A. Klimas, N. Zhao, Y. Zhao, S.-C. Chen, *Science* **2022**, *378*, 1325.
- [117] D. Oran, S. G. Rodrigues, R. Gao, S. Asano, M. A. Skylar-Scott, F. Chen, P. W. Tillberg, A. H. Marblestone, E. S. Boyden, *Science* **2018**, *362*, 1281.
- [118] M. Sharipova, T. Baluyan, K. Abrashitova, G. Kulagin, A. Petrov, A. Chizhov, T. Shatalova, D. Chubich, D. Kolymagin, A. Vitukhnovsky, V. Bessonov, A. Fedyanin, *Opt. Mater. Express* **2021**, *11*, 371.
- [119] S. Varapnickas, S. Chandran Thodika, F. Moroté, S. Juodkakis, M. Malinauskas, E. Brasselet, *Appl. Phys. Lett.* **2021**, *118*, 151104.
- [120] U. T. Sanli, H. Ceylan, I. Bykova, M. Weigand, M. Sitti, G. Schütz, K. Keskinbora, *Adv. Mater.* **2018**, *30*, 1802503.
- [121] H. Schiff, R. Kirchner, N. Chidambaram, M. Altana, in *Nanophotonics Australasia 2017*, Vol. 10456. SPIE, Paris, **2018**, pp. 39–47.
- [122] B. Jia, J. Serbin, H. Kim, B. Lee, J. Li, M. Gu, *Appl. Phys. Lett.* **2007**, *90*, 073503.
- [123] B. Buchegger, J. Kreutzer, B. Plochberger, R. Wollhofen, D. Sivun, J. Jacak, G. J. Schütz, U. Schubert, T. A. Klar, *ACS Nano* **2016**, *10*, 1954.
- [124] M. Elmeranta, G. Vicidomini, M. Duocastella, A. Diaspro, G. de Miguel, *Opt. Mater. Express* **2016**, *6*, 3169.
- [125] S. D. Gittard, A. Nguyen, K. Obata, A. Koroleva, R. J. Narayan, B. N. Chichkov, *Biomed. Opt. Express* **2011**, *2*, 3167.
- [126] G. Vizsnyczai, L. Kelemen, P. Ormos, *Opt. Express* **2014**, *22*, 24217.
- [127] R. Nielson, B. Kaehr, J. B. Shear, *Small* **2009**, *5*, 120.
- [128] H. Wang, W. Zhang, D. Ladika, H. Yu, D. Gailevicius, H. Wang, C.-F. Pan, P. N. S. Y. Ke, T. Mori, J. Y. E. Chan, Q. Ruan, M. Farsari, M. Malinauskas, S. Juodkakis, M. Gu, J. K. Yang, *Adv. Funct. Mater.* **2023**, 2214211 <https://doi.org/10.1002/adfm.202214211>
- [129] J. A. Kim, D. J. Wales, A. J. Thompson, G.-Z. Yang, *Adv. Opt. Mater.* **2020**, *8*, 1901934.
- [130] Y. Qi, S. Zhang, S. Feng, X. Wang, W. Sun, J. Ye, P. Han, Y. Zhang, In *2017 Int. Conf. on Opt. Instr. and Technol: IRMMW-THz Technologies and Applications*, Vol. 10623. SPIE, Paris, **2018**, pp. 203–208.
- [131] D. Gonzalez-Hernandez, S. Varapnickas, G. Merkininkaitė, A. Čiburys, D. Gailevičius, S. Šakirzanovas, S. Juodkakis, M. Malinauskas, in *Photonics*, Vol. 8. MDPI, Basel, Switzerland, **2021**, pp. 577.
- [132] A. Butkutė, L. Čekanavičius, G. Rimšelis, D. Gailevičius, V. Mizeikis, A. Melninkaitis, T. Baldacchini, L. Jonušauskas, M. Malinauskas, *Opt. Lett.* **2020**, *45*, 13.
- [133] D. Gailevicius, R. Zvirblis, M. Malinauskas, *to be published 2023, under review*.
- [134] S. Ristok, S. Thiele, A. Toulouse, A. M. Herkommer, H. Giessen, *Opt. Mater. Express* **2020**, *10*, 2370.
- [135] A. Žukauskas, G. Batavičiūtė, M. Ščiuka, T. Jukna, A. Melninkaitis, M. Malinauskas, *Opt. Mater. Express* **2014**, *4*, 1601.
- [136] H. Wang, H. Wang, W. Zhang, J. K. Yang, *ACS Nano* **2020**, *14*, 10452.
- [137] K. Weber, F. Hütt, S. Thiele, T. Gissibl, A. Herkommer, H. Giessen, *Opt. Express* **2017**, *25*, 19672.
- [138] M. Power, A. J. Thompson, S. Anastasova, G.-Z. Yang, *Small* **2018**, *14*, 1703964.
- [139] M. Zou, C. Liao, S. Liu, C. Xiong, C. Zhao, J. Zhao, Z. Gan, Y. Chen, K. Yang, D. Liu, Y. Wang, Y. Wang, *Light Sci. Appl.* **2021**, *10*, 171.
- [140] G. Merkininkaitė, D. Gailevicius, L. Stasiunas, E. Ezerskyte, R. Vargalis, M. Malinauskas, S. Sakirzanovas, *to be published 2023, under review*.
- [141] A. Albiez, R. Schwaiger, *MRS Adv.* **2019**, *4*, 133.
- [142] M. Diamantopoulou, N. Karathanasopoulos, D. Mohr, *Addit. Manuf.* **2021**, *47*, 102266.
- [143] T. Gissibl, S. Wagner, J. Sykora, M. Schmid, H. Giessen, *Opt. Mater. Express* **2017**, *7*, 2293.
- [144] J.-g. Liu, M. Ueda, *J. Mater. Chem.* **2009**, *19*, 8907.
- [145] S. Song, Y. Li, Z. Yao, J. Li, X. Li, Y. Cao, *Nanomaterials* **2021**, *12*, 55.
- [146] M. Deubel, G. Von Freymann, M. Wegener, S. Pereira, K. Busch, C. M. Soukoulis, *Nat. Mater.* **2004**, *3*, 444.
- [147] N. Tétreault, G. von Freymann, M. Deubel, M. Hermatschweiler, F. Pérez-Willard, S. John, M. Wegener, G. A. Ozin, *Adv. Mater.* **2006**, *18*, 457.
- [148] H. Ren, J. Jang, C. Li, A. Aigner, M. Plidschun, J. Kim, J. Rho, M. A. Schmidt, S. A. Maier, *Nat. Commun.* **2022**, *13*, 4183.
- [149] L. Siegle, S. Ristok, H. Giessen, *Opt. Express* **2023**, *31*, 4179.
- [150] J. Bauer, A. G. Izard, Y. Zhang, T. Baldacchini, L. Valdevit, *Opt. Express* **2020**, *28*, 20362.
- [151] D. Gonzalez-Hernandez, B. Sanchez-Padilla, D. Gailevičius, S. C. Thodika, S. Juodkakis, E. Brasselet, M. Malinauskas, *Adv. Opt. Mater.* **2023**, 2300258 <https://doi.org/10.1002/adom.202300258>
- [152] M. Schmid, D. Ludescher, H. Giessen, *Opt. Mater. Express* **2019**, *9*, 4564.
- [153] T. Aderneuer, O. Fernández, R. Ferrini, *Opt. Express* **2021**, *29*, 39511.
- [154] X. Chen, T. Sun, F. Wang, *Chem. Asian J* **2020**, *15*, 21.
- [155] A. Žukauskas, M. Malinauskas, L. Kontenis, V. Purlys, D. Paipulas, M. Vengris, R. Gadonas, *Lith. J. Phys.* **2010**, *50*, 1.
- [156] B. Henderson, *Contemporary Phys.* **2002**, *43*, 273.
- [157] A. J. Otuka, N. B. Tomazio, K. T. Paula, C. R. Mendonça, *Polymers* **2021**, *13*, 1994.
- [158] T. Reynolds, N. Riesen, A. Meldrum, X. Fan, J. M. Hall, T. M. Monro, A. François, *Laser Photonics Rev.* **2017**, *11*, 1600265.
- [159] A. W. Schell, J. Kaschke, J. Fischer, R. Henze, J. Wolters, M. Wegener, O. Benson, *Sci. Rep.* **2013**, *3*, 1577.
- [160] C. Arnoux, L. A. Pérez-Covarrubias, A. Khaldi, Q. Carlier, P. L. Baldeck, K. Heggarty, A. Banyasz, C. Monnereau, *Addit. Manuf.* **2022**, *49*, 102491.
- [161] E. H. Waller, G. Von Freymann, *Polymers* **2016**, *8*, 297.
- [162] I. S. Ladner, M. A. Cullinan, S. K. Saha, *RSC Adv.* **2019**, *9*, 28808.
- [163] T. Grossmann, S. Schleede, M. Hauser, T. Beck, M. Thiel, G. Von Freymann, T. Mappes, H. Kalt, *Opt. Express* **2011**, *19*, 11451.
- [164] A. Brooks, X.-L. Chu, Z. Liu, R. Schott, A. Ludwig, A. D. Wieck, L. Midolo, P. Lodahl, N. Rotenberg, *Nano Lett.* **2021**, *21*, 8707.
- [165] S. Ristok, P. Flad, H. Giessen, *Opt. Mater. Express* **2022**, *12*, 2063.
- [166] K. Galvanauskas, D. Astrauskyte, G. Balcas, D. Gailevicius, L. Grineviciute, M. Malinauskas, *Optica Open* **2023** Preprint; <https://doi.org/10.1364/opticaopen.22302655.v1>.
- [167] M. D. Schmid, A. Toulouse, S. Thiele, S. Mangold, A. M. Herkommer, H. Giessen, *Adv. Funct. Mater.* **2022**, 2211159.
- [168] A. Toulouse, S. Thiele, H. Giessen, A. M. Herkommer, *Opt. Lett.* **2018**, *43*, 5283.

- [169] K. Weber, Z. Wang, S. Thiele, A. Herkommer, H. Giessen, *Optics Letters* **2020**, *45*, 2784.
- [170] W. Duan, X. Yin, Q. Li, L. Schlier, P. Greil, N. Travitzky, *J. Eur. Ceram. Soc.* **2016**, *36*, 3681.
- [171] J. Schmidt, L. Brigo, A. Gandin, M. Schwentenwein, P. Colombo, G. Brusatin, *Addit. Manuf.* **2019**, *30*, 100913.
- [172] D. Wu, S.-Z. Wu, J. Xu, L.-G. Niu, K. Midorikawa, K. Sugioka, *Laser Photonics Rev.* **2014**, *8*, 458.